IBP1340_18

WATER INJECTION DYNAMIC MODEL FOR PRESSURE INSTABILITIES INVESTIGATION

Álvaro M. Borges Filho[1], Kamila S. Oliveira[2], Rodrigo S. Monteiro[3], Ana Cristina B. Garcia[4], Fernando B. Pinto[5].

Abstract

The opening of the wells at the startup of a water injection system for offshore production platforms can cause oscillations in the flow, pressure and level system control loops. Those oscillations can reach unacceptable frequencies and amplitudes for the integrity of the equipment. To evaluate the oscillations causes and to test solutions, a dynamic computational model was developed. This work describes the methodology used for the system modeling, the tests performed, the diagnoses and solutions found. The computational simulation proved to be an effective method for investigating anomalies in the system behavior and creates the possibility of testing solution proposals, avoiding risks of undesired shutdowns in the platform operation.

Keywords: Petroleum. Production. Water injection system. Control system. Dynamic computational modeling.

1. Introduction

The water injection system on offshore production platforms for secondary recovery consists basically of the treatment of the water taken up at sea and pumping it, at high pressure, to injection wells. At system startup, the opening of the wells can cause oscillations in the flow, pressure and level control loops. Those oscillations can reach unacceptable frequencies and amplitudes for the integrity of the equipment and may cause the system to shut down. For evaluating oscillations causes and testing solutions, a dynamic computational simulator was developed.

The objective of this work is to describe the methodology of construction of this simulator, the tests performed, the diagnoses and solutions found. The simulations were implemented in Simulink environment, in MATLAB R2017b software.

[1]M.Sc., Automation Engineer - ILTC
[2]M.Sc., Chemistry – ADDLabs/UFF
[3]D.Sc., Computer Science – ADDLabs/UFF
[4]Ph.D., Computer Aided Civil Engineering – UNIRIO/CCET
[5]M.Sc., Administration – ADDLabs/UFF

2. System Description

The studied water injection system is composed of seven control loops, being the corresponding controllers named as LIC-01, FIC-01, FIC-02, FIC-03, XC-01, PIC-01 and PIC-W, where one is used for level, three for flow, one for valve position and two for pressure.

Although the studied water injection system has many subsystems, the region of interest of this analysis lies between the deaerator vessel and the injection riser, including the booster and main pumps.

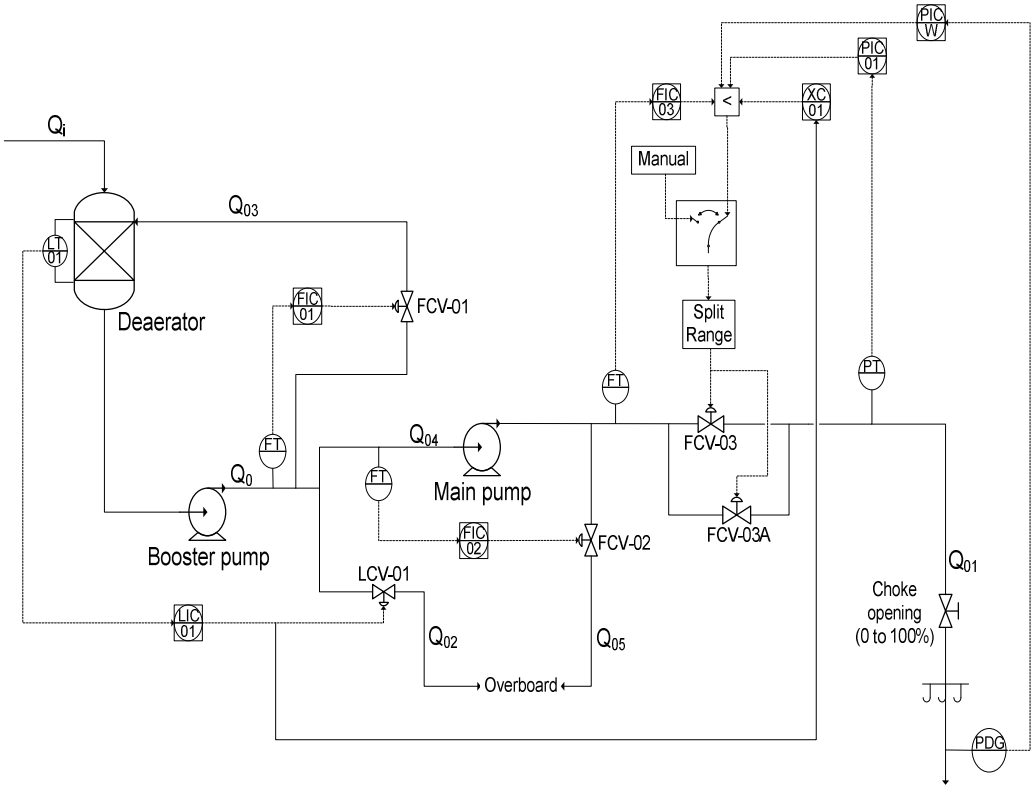

Figure 1. Water injection process control diagram

3. Modeling the System Components

Based on the P&IDs (Piping and Instrumentation Diagram) of the water injection system mentioned, the Process Control Diagram was elaborated as depicted in Figure 1. Next, the System Block Diagram was built to represent it dynamically. This diagram is formed by the transfer functions of each element of the system, such as sensors, controllers, valves, vessels, pumps and pipes (Seborg et al., 1989). The system was modeled in stages, adding to the Block Diagram each control loop at a time and testing for validation. Figure 2 shows the final stage with all the control loops.

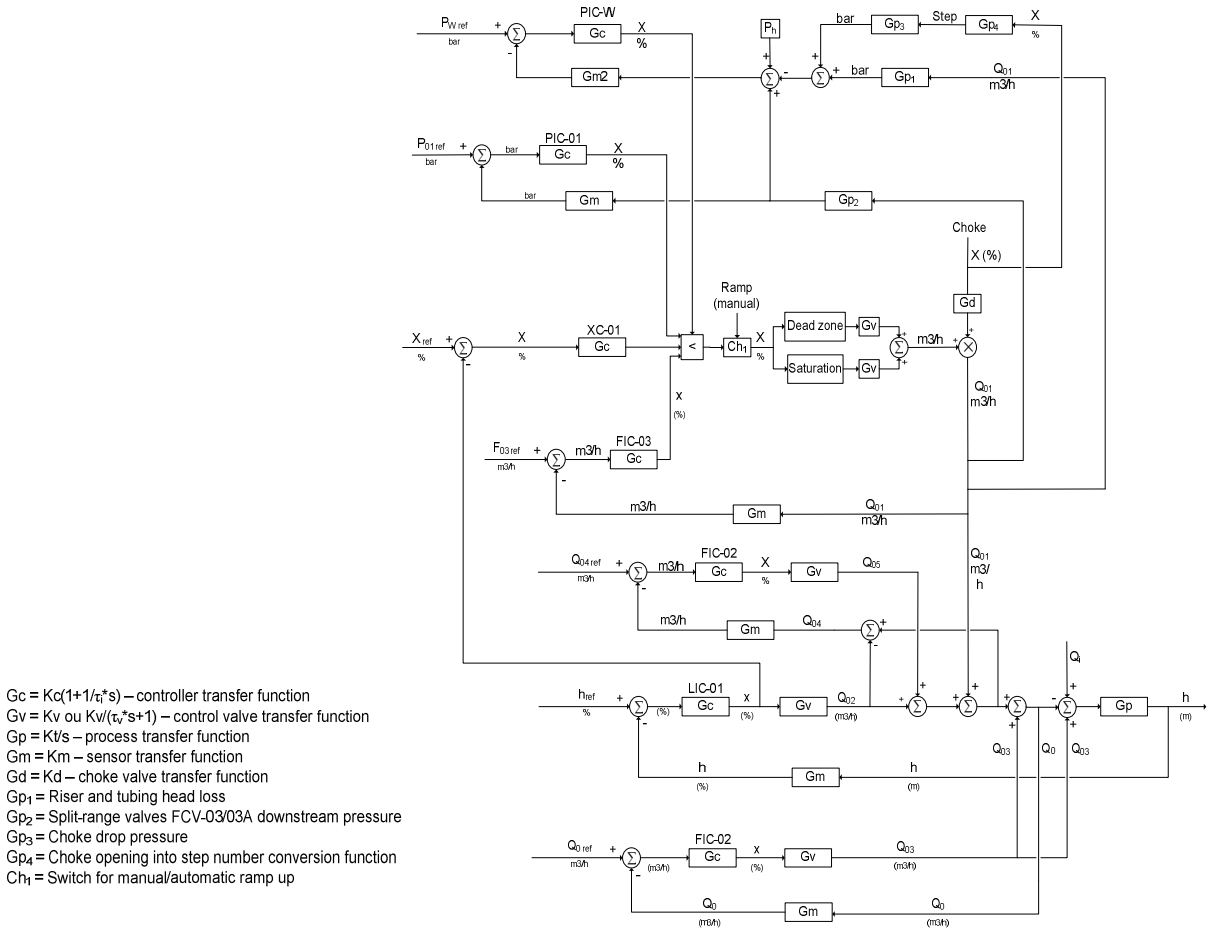

Gc = Kc(1+1/τ_i*s) – controller transfer function
Gv = Kv ou Kv/(τ_v*s+1) – control valve transfer function
Gp = Kt/s – process transfer function
Gm = Km – sensor transfer function
Gd = Kd – choke valve transfer function
Gp_1 = Riser and tubing head loss
Gp_2 = Split-range valves FCV-03/03A downstream pressure
Gp_3 = Choke drop pressure
Gp_4 = Choke opening into step number conversion function
Ch_1 = Switch for manual/automatic ramp up

Figure 2. Water injection system block diagram

3.1. Level and Flow Modeling

The modelling procedure was started by the level and flow loops, applying mass balance based on the inlet flow in the deaerator and the outlet flow to the injection wells and to overboard. The next step was to define the transfer functions to represent the dynamic of each component of the system. The parameters of each transfer function were calculated from equipment and instruments datasheets and design information.

The transfer function of the vessel and booster pump assembly, $G_p(s)$, was modeled as an integrating system. Its input is the balance of flows that feed and leave the vessel ($Q(s)$) and the output is the vessel level ($L(s)$) (Campos et al., 2006) as shown in Equation 1.

$$G_p(s) = \frac{L(s)}{Q(s)} = \frac{K_t}{s} \tag{1}$$

The gain K_t was obtained using the vessel volume and inlet flow, Δu, to calculate the filling time, Δt, and the range level, Δy, in Equation 2.

$$K_t = \frac{\Delta y}{\Delta t} \times \frac{1}{\Delta u} \tag{2}$$

The controllers transfer functions, $G_c(s)$, were modeled with Proportional and Integral actions, as shown in Equation 3. The proportional gain K_c and integral gain τ_i values were equal to the used in the platform.

$$G_c(s) = \frac{X(s)}{E(s)} = K_c \times \left(1 + \frac{1}{\tau_i\, s}\right) \tag{3}$$

The transfer functions of the level, flow and pressure sensors, $G_m(s)$, were modeled by a simple gain, as shown in Equation 4. The down hole pressure sensor (PDG), $G_{m\,PDG}(s)$, was modeled as a first order system with dead time due to the delay in signal transmission, according to Equation 5. All the gains equal to one except for the level transmitter that needs to transform the engineering units from meter to %.

$$G_m(s) = \frac{Y(s)}{U(s)} = K_m \tag{4}$$

$$G_{m\,PDG}(s) = \frac{K_m\; e^{-\theta_m s}}{\tau_m\, s + 1} \tag{5}$$

The control valves were modeled as first order systems, the input is the opening signal ($X(s)$) and the output is the flow ($Q(s)$) (Smith and Corripio, 2008), as depicted in Equation 6.

$$G_v = \frac{Q(s)}{X(s)} = \frac{K_v}{\tau_v\, s + 1} \tag{6}$$

The time constants τ_v were calculated considering 63% of the valve full travel time, estimated as 1 second for each inch of diameter. The gains K_v were considered constant for valves LCV-01, FCV-01, FCV-02 and FCV-03, and each value was determined according to the maximum flow informed in the respective valve datasheet. For valve FCV-03A the gain was considered variable and was obtained from field historical data as shown in Figure 3.

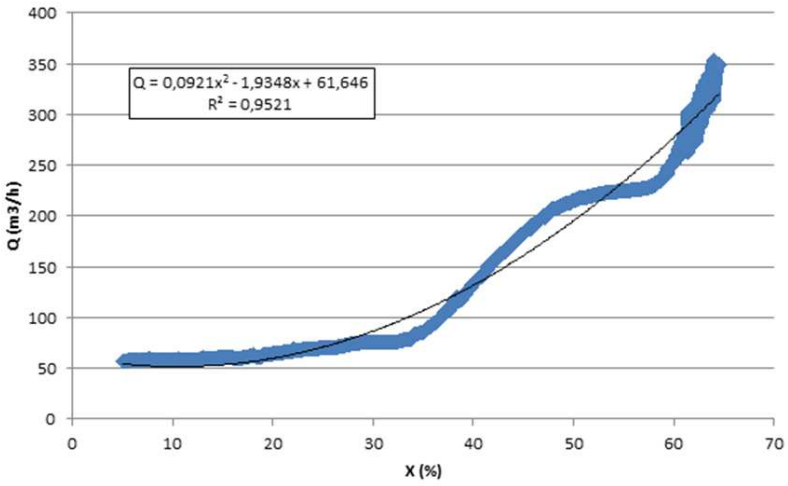

Figure 3. Model of FCV-03A gain based on field historical data

3.2. Pressure Modeling

All the pressures were modeled from the flow values considering the pressure drop in pipes and valves, hydrostatic pressure and pump outlet pressure. The dynamic in the pressures models was not considered since the system uses incompressible fluid and steal piping. The main centrifugal pump discharge pressure was modeled as a first order polynomial, determined by an approximation from the pump performance curve as show in Equation 7.

$$P = \left(\frac{P_{min} - P_{max}}{Q_{max}}\right) Q + P_{max} \tag{7}$$

The pressure PT-01, downstream the control valve FCV-03A, was modeled as a first order polynomial using field historical data from PT-01 and FT-03, as shown in Figure 4.

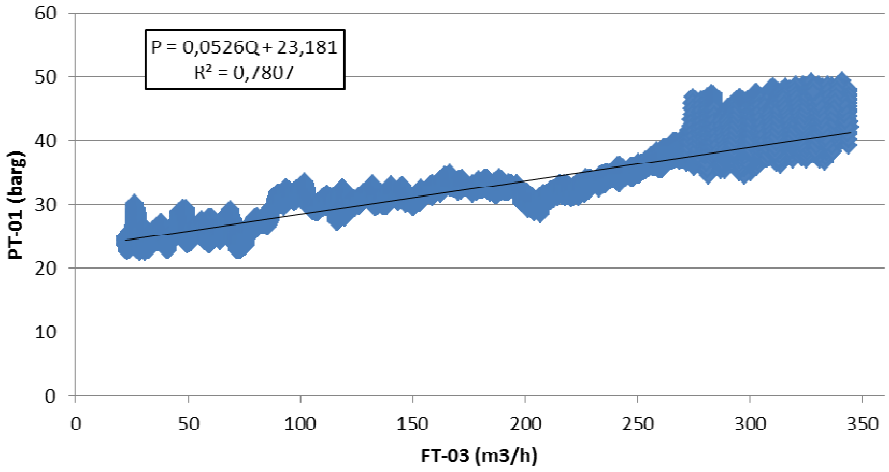

Figure 4. PT-01 pressure model based in FT-03 and PT-01 historical field data

For modeling the PDG pressure it was necessary to add the hydrostatic pressure to the value of PT-01 model and subtract de pressure drop in pipes and choke valve. The hydrostatic pressure, P_h, was calculated by Equation 8, where h is vertical distance between PT-01 and the PDG.

$$P_h = \rho g h \tag{8}$$

The pressure drop, P_{pc}, in each pipe segment, such as risers and tubing, was modeled as a second-order polynomial function of flow, determined from concepts of Fluid Mechanics (Husu et al., 1994), as shown in Equations 9 and 10, where λ is the friction factor obtained from the Moody diagram, using the Reynolds number and pipe relative roughness.

$$P_{pc} = K_{pc} \times Q^2 \tag{9}$$

$$K_{pe} = \frac{8 \times \lambda \times L \times \rho}{\pi^2 \times D^5} \tag{10}$$

The pressure drop in the subsea choke valve, P_{ch}, was modeled as a first order polynomial, as shown in Figure 5.a, obtained by the difference between field historical data from subsea pressure transmitters installed upstream and downstream the choke valve respectively, versus choke step number. To change the opening choke valve engineering unit from % to step number it was used the function plotted in Figure 5.b obtained from valve vendor data.

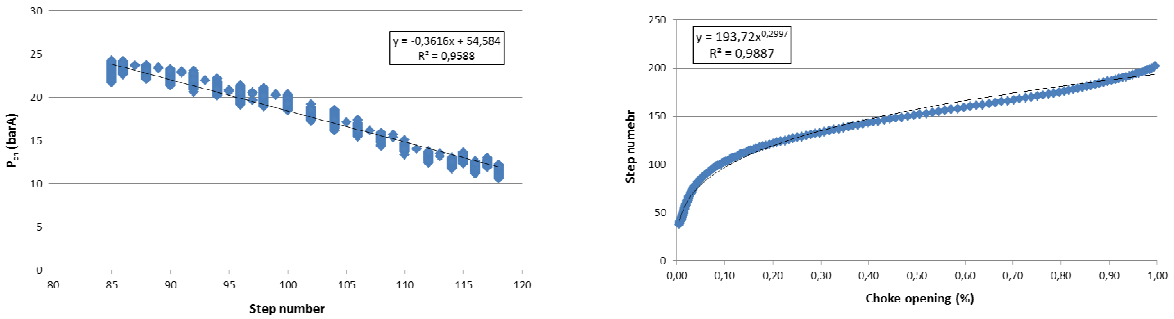

(a) (b)

Figure 5. (a) Model of the pressure drop in choke valve as a function of the step number obtained from field historical data. (b) Percent opening choke valve as a function of step number.

Putting together the pressure models above, the Equation 11 models PDG pressure, where $K_{pe\_sec\_n}$ shall be determined for each pipe segment using Equations 9 and 10.

$$P_{PDG} = PT_{01} + P_h - \left(K_{pe\_sec\_2} \times Q^2\right) - \left(K_{pe\_sec\_3.1} \times Q^2\right) - \left(K_{pe\_sec\_3.4.5} \times \left(\frac{3}{4} \times Q\right)^2\right) - \left(K_{pe_{tubing}} \times (1/4 \times Q)^2\right) - P_{ch} \tag{11}$$

3.3. Noise Cavitation Modeling

The comparison between pressure and flow field historical data with information from the main injection valve FCV-03A datasheet led to the conclusion that it operates above its design capacity and can be cavitating and producing a flow noise that can cause instability in the control loops.

According to Ulanickia et al. (2016) and ISA-RP75.23 (1995), cavitation can be predicted by the dimensionless index σ_{ISA}. Figure 6.a shows the equation to calculate the cavitation index, where P1 and P2 are the upstream and downstream pressure respectively and Pv is the vapor pressure of the fluid. Maximum vibration occurs in the region of low values of σ_{ISA}, near 1. Figure 6.b shows the curve of the calculated index for a wide range of FCV-03A valve opening, based in historical field data, and can be observed that σ_{ISA} varies from 1.175 to 1.45.

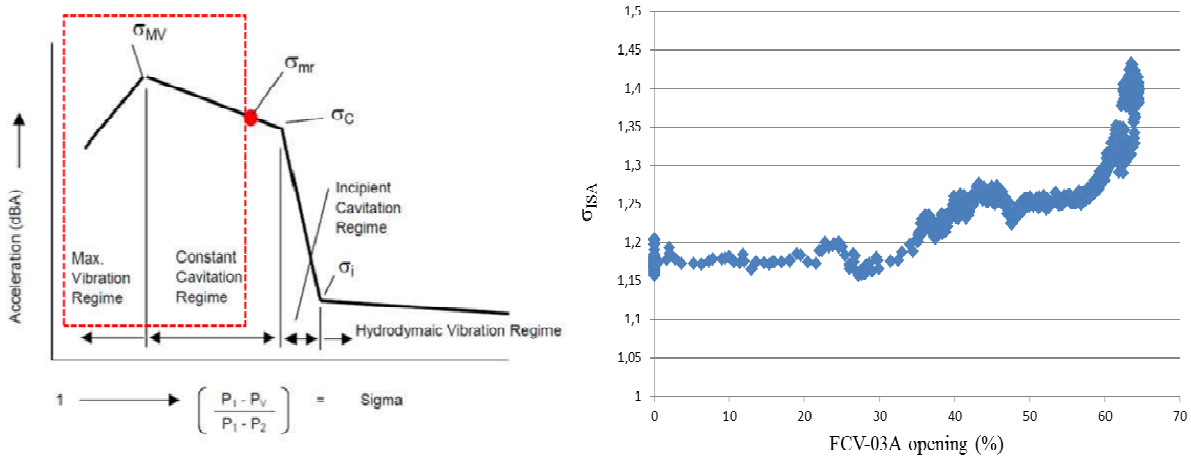

Figure 6. (a) Relation between vibration and cavitation index σ_{ISA} in a tipical control valve. The probable region of FCV-03A operation is highlighted in the red rectangle. (b) Relation between FCV-03A opening and cavitation indices σ_{ISA} calculated from historical field data

It can be inferred from Figure 6.a and 6.b that FCV-03A is operating in the "Maximum Vibration" and the "Constant Cavitation" regimes. Therefore, it is expected that the noise level (acceleration) will increase and then decrease as the valve goes from closed to full opened, and that it can be modeled more by a variation of frequency than of amplitude.

According to Liptak et al. (1995) and Roth and Stares (2001), cavitation, despite being a phenomenon with frequency ranging from 100 to 10.000 Hz occurring downstream, it can cause low frequency movement of the valve assembly: plug, stem and actuator, especially in the case of diaphragm type actuators. For "flow to open globe valves", this low frequency vibration can propagate to upstream and resonate with the piping.

To simulate this phenomenon, a simplified cavitation noise model was added to the position command of the FCV-03A valve. The noise was modeled in the form of three different sinusoids of high (10 rd/s), medium (0,1 rd/s) and low (0,001 rd/s) frequencies, with amplitude of 2%, switched by the valve opening command signal (60 and 64%) as shown in Figure 7.

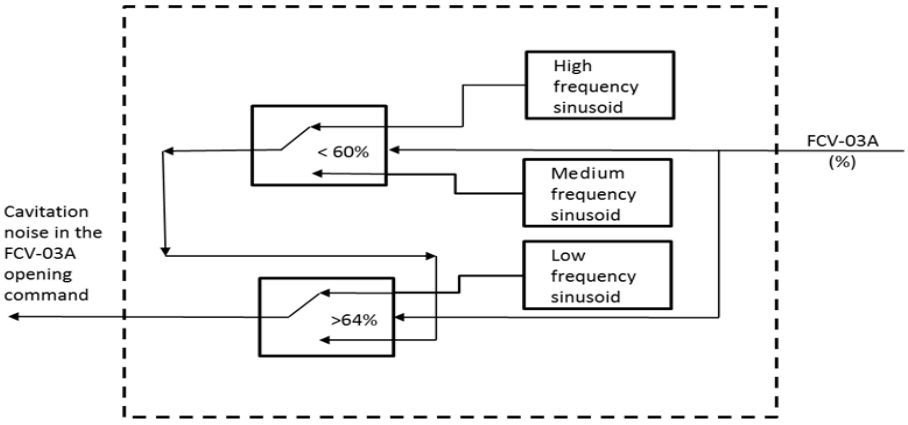

Figure 7. Three-frequency model for the cavitation noise

The level and flow measurement noise, caused by the platform movement due to maritime waves, were also modeled as sinusoids of low frequency (1,2 and 0,628 rd/s respectively).

3.4. Symulink Dynamic System Model

With all the transfer functions defined and parameterized in the Block Diagram, the Dynamic System Model was configured using the Simulink/Matlab environment. Figure 8 shows part of the model that includes the control loops LIC-01, FIC-01 and FIC-02, the level, flow and cavitation noises and the set of injection valves FCV-03/03A operating in split-range.

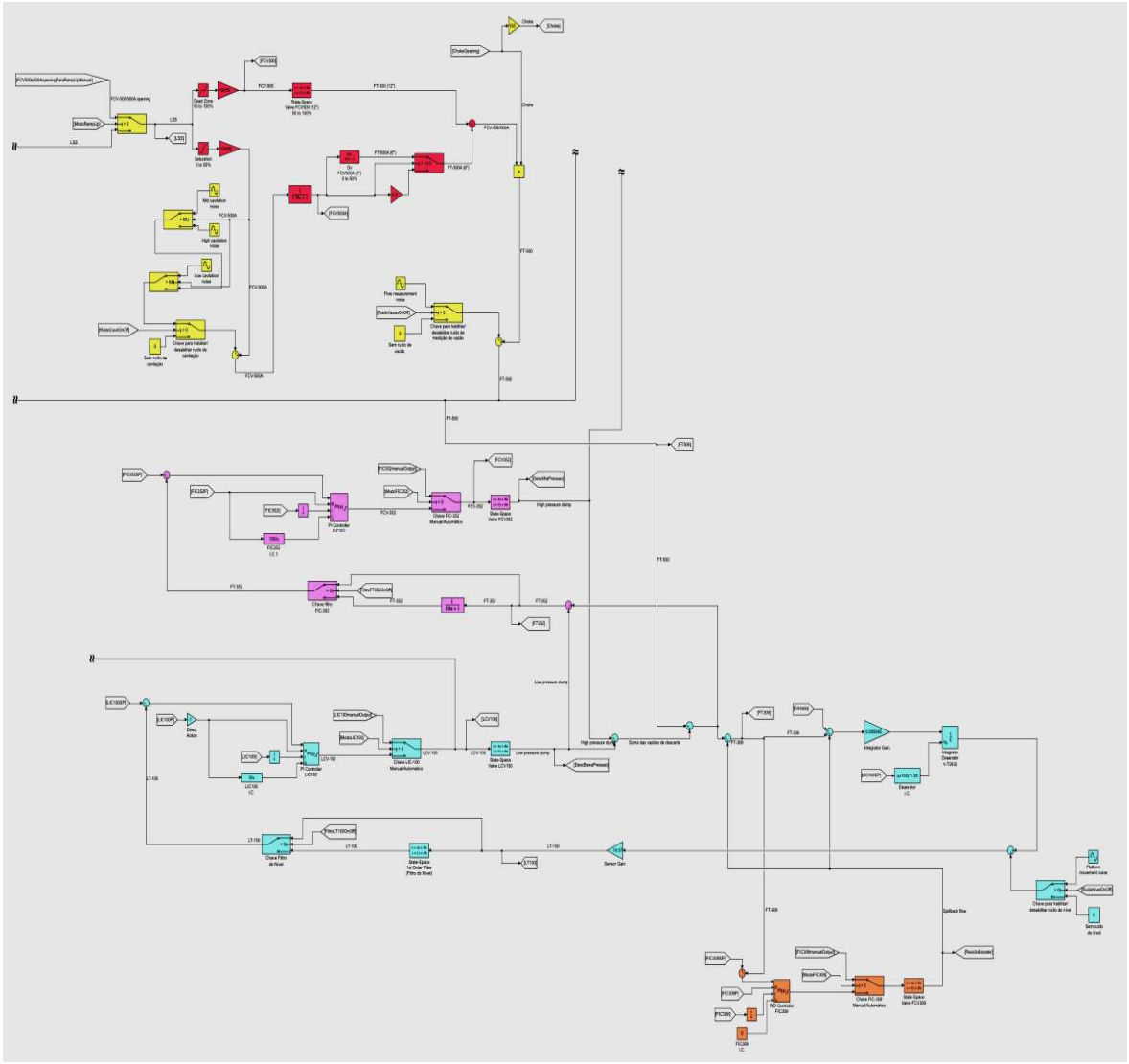

Figure 8. Part of the Simulink/Matlab water injection system model

4. Procedure of the Simulations

The simulations were performed according to a test procedure for validating the model and enabling the observation of conditions that favor the emergence of instabilities in the system (Borges et al., 2014).

The tests were designed to investigate hypotheses of typical causes of oscillations in control systems, such as inadequate tuning of controllers, interaction between control loops, sensor measurement noises, nonlinearities in valves, valve and pumps cavitation, dead time in sensors and valve bump on the transfer of controllers operating in override.

Initially, the controllers were configured with the parameters currently used in the platform, in order to represent the actual operating conditions. The results of the simulations were compared with historical operational data, thus allowing the validation of the model. After that, several controller parameter values were tested to obtain a stable behavior of the system.

5. Results

The simulation of a ramp up procedure (system startup by opening the injection wells) was done to investigate the pressure and flow oscillations observed in historical data showed in Figure 9. The controllers FIC-03, XC-01, PIC-01 and PIC-W that actuate in override were operating in manual mode and only the split-range valve FCV-03A was being used.

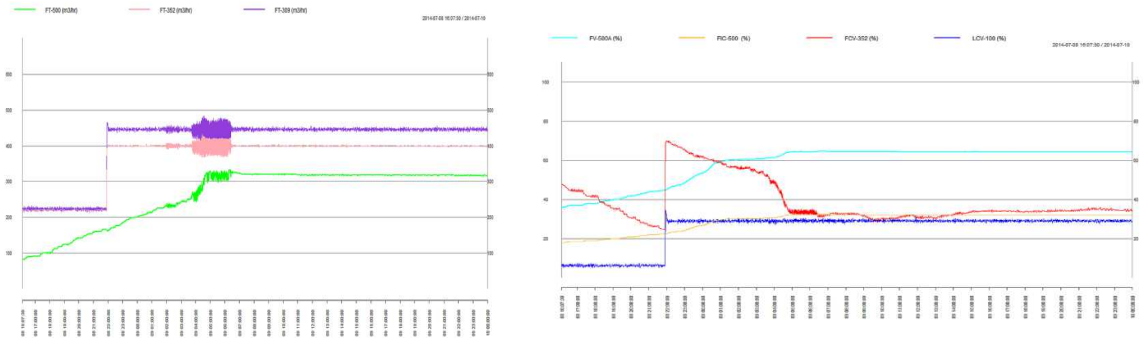

(a) (b)

Figure 9. Historical data of flows (a) and controllers outputs (b) showing oscillations during the ramp up.

The simulation depicted in Figure 10 is very similar to the ramp up historical data, shown in Figure 9, and demonstrate the accuracy of the computational model. A series of other simulations showed a strong coupling between the level controller LIC-01 and the flow controller FIC-02. The simulation of cavitation noise in the FCV-03A valve causes the flow measured by the sensor FT-02 to be noisy, introducing more oscillation by the FIC-02 controller action on FCV-02 valve.

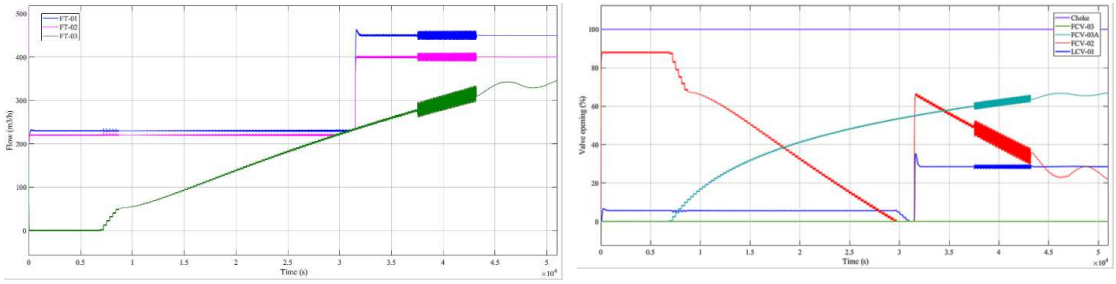

(a) (b)

Figure 10. Flows (a) and controllers outputs (b) simulations using tuning parameters currently used in the platform.

To obtain a new tuning parameters for controller FIC-02, with the objective to decouple it from controller LIC-01 and to reject cavitation noise, it was simulated the injection of a range of cavitation noise frequencies and measured the amplitude of FT-02, as shown in Figure 11.

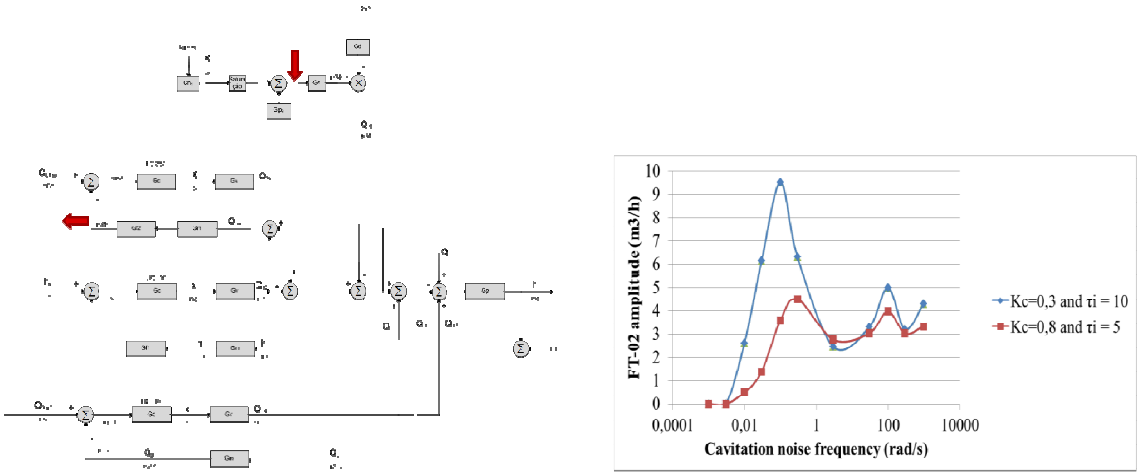

(a) (b)

Figure 11. (a) Water Injection System Model used to inject cavitation noise at FCV-03A and measure FT-02 amplitude. (b) Gain Diagram of FT-02 amplitude before and after FIC-02 tuning.

A ramp up simulation with the new tuning parameters of the FIC-02 controller ($K_c = 0.8$ and $\tau_i = 5$) showed an overall reduction of the oscillations, which can be observed comparing Figures 10 and 12.

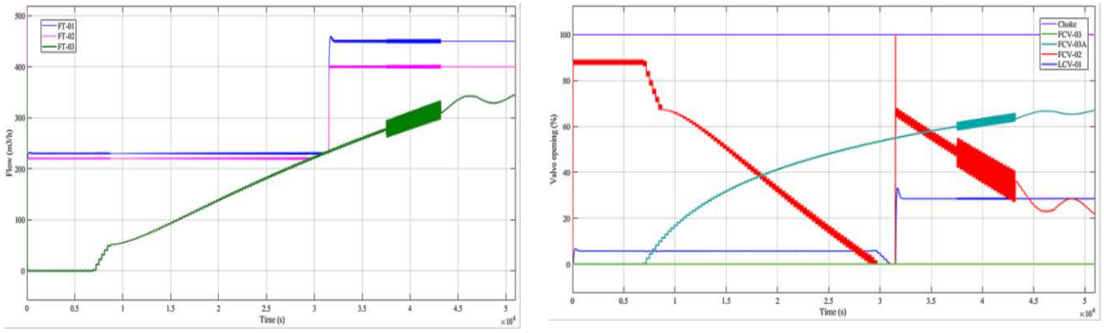

(a) (b)

Figure 12. (a) Flows and (b) controllers outputs simulations after tuning.

It can be observed that the amplitude of FT-01 and FT-02 were largely reduced, however the amplitude of FT-03 and of FCV-03A had a very small reduction due to the noise being directly added to the valve position and the valve FCV-03A being in manual. The amplitude of valve LCV-01 opening was reduced, but the amplitude of FCV-02 opening increased in other to reduce the flows oscillations.

6. Conclusions

The construction of a dynamic model of the water injection control system and the execution of a simulated test set constitute an effective method for investigating anomalies in the behavior of the system during the wells opening. The possibility of testing solution proposals in the simulator avoided risks of undesired shutdowns in platform operation.

7. Acknowledgements

The authors are grateful to Shell for sponsoring this research and the ANP (Brazil's National Oil, Natural Gas and Biofuels Agency) for the strategic importance of the support given through the R&D levy regulation.

8. References

BORGES, A. M.; PASSARIN, T. A. R.; CHULEK, M. J. Tuning of the Pressure Controllers of a Petroleum Production Plant to Reduce Gas Burning. In: 4th PETROBRAS INSTRUMENTATION, CONTROL AND AUTOMATION CONGRESS (CICAP), 2014.

CAMPOS, M. C. M. M.; TEIXEIRA, H. C. G. *Typical Controls of Industrial Equipment and Processes*: Editor Edgar Blucher, 2006.

HUSU, M. et al. *Flow Control Manual*: Neles-Jamesbury, 1994.

ISA-RP75.23-1995 - Recommended Practice, Considerations for Evaluating Control Valve Cavitation.

LIPTAK, B. G. Instrument Engineers' Handbook, Fourth Edition, Volume Two: *Process Control and Optimization*, Page. 1217

ROTH, K. W.; STARES, J. A. Avoid control valve application problems with physics-based models - Kinetic energy criteria have many limitations: HYDROCARBON PROCESSING, August 2001.

SEBORG, D. E.; EDGAR, T. F.; MELLICHAMP, D. A. *Process Dynamics and Control*: 1. ed.: John Wiley and Sons, Inc., 1989.

SMITH, C. A.; CORRIPIO, A. *Princípios e Prática do Controle Automático de Processo*: 3. ed. Rio de Janeiro: LTC Editora, 2008.

ULANICKIA B.; PICINALIB L.; JANUSA T. *Measurements and analysis of cavitation in a pressure reducing valve during operation – a case study*: Published by Elsevi, 2016.